International Journal for Modern Trends in Science and Technology, 9(01): 16-23, 2023

ISSN: 2455-3778 online
DOI: https://doi.org/10.46501/IJMTST0901003
Available online at: http://www.ijmtst.com/vol9issue01.html

Bio Convective Flow of the Tangent-Hyperbolic Nano fluid Past a Flat Surface

Farah Rizwan[1] | Dr. Rashid Mehmood[2]

[1]Mathematics, HITEC University, Taxila, Rawalpindi, Pakistan
[2]Mathematics, HITEC University, Taxila, Rawalpindi, Pakistan

To Cite this Article
Farah Rizwan and Dr. Rashid Mehmood. Bio Convective Flow of the Tangent-Hyperbolic Nano fluid Past a Flat Surface. International Journal for Modern Trends in Science and Technology 2022, 9(01), pp. 16-23. https://doi.org/10.46501/IJMTST0901003

Article Info
Received: 20 December 2022; Accepted: 11 January 2023; Published: 14 January 2023.

ABSTRACT

There are many important applications of boundary layer flow of the nano fluids over the stretching sheet in manufacturing processes. A nanofluid is basically the mixture of nano particles contained in base fluid like water, glycol, and ethylene etc. nanofluid helps to improve the fluid's thermal conductivity and also increases the rate of transfer of heat. In this research gyrotactic microorganisms are added along with nano particles within the base fluid. The governing problem flow is tackled numerically to explore velocity F′(η), temperature θ(η), concentration φ(η), motile microorganism density ξ(η), Nusselt number 〖 Nu〗_x, Sherwood number 〖 Sh〗_x and local Motile microorganism density parameter 〖 Nn〗_x against pertinent physical parameters. Figure IV.10 and IV.11 is showing the results with various researches and it is showing the exact agreement with the paper results.

1. INTRODUCTION

Let us consider a two-dimensional unsteady and incompressible flow of fluid due to the stretching sheet. Thetransfer of heat of tangent-hyperbolic fluid along the wall is with the plane y=0. Fluid flow which is under consideration is at y>0. Velocity of stretching sheet is U_w and temperature at surface is T_w . A magnetic field having constant strength B_0 is applied perpendicularly to the stretching sheet and magnetic field that is induced is so small that it can be neglected. Unsteady flow of the fluid and transfer of heat starts at time t=0. The geometry of the problem is shown in figure I.1.

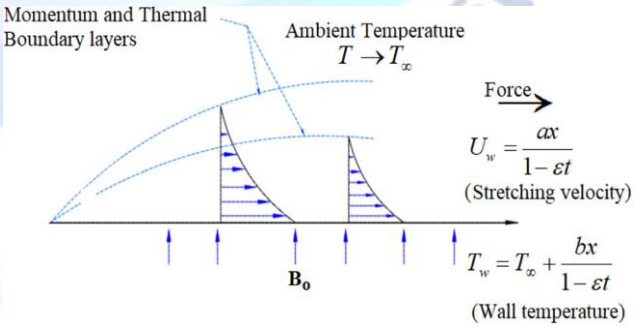

Figure 0-1: Geometry of the problem

2. LITERATURE REVIEW

There are many important applications of boundary layer flow of the nano fluids over the stretching sheet in manufacturing processes. A nanofluid is basically the mixture of nano particles contained in base fluid like water, glycol, and ethylene etc. nanofluid helps to

improve the fluid's thermal conductivity and also increases the rate of transfer of heat. Nanofluids are formed because of the dispersion of nano-meter substance within the base fluid. Besthapu et. al. [1] discussed the effect of viscous dissipation of flow of mixed convection which is thermally stratifying MHD nanofluid over stretching surface. Sheikholeslami et. al. [2] presented the flow of magnetic nano fluid and the convective transfer of heat in a porous cavity. Sheikholeslami [3] explored the numerical approach for transportation of MHD Al2O3–water nano fluid in permeable medium.

Nowadays bio convective nanofluids over the stretching sheet are attracting the researches around the world due to its vast industrial applications such as biotechnology because they have great mixing property and increases the transport of mass. Density gradient of motile microorganisms is behind occurrence of bioconvection. The microorganisms can swim easily and actively in the base fluid. The parameters like gravity, oxygen gradient, intensity of light and chemical substance are very helpful for microorganisms so that they may be able to swim easily in the upward direction. Sheikholeslami [4] presented the computational approach for entropy and energy analysis of nanofluid acting under influence of Lorentz force acting on a porous medium. Aftab et. al. [5] discussed the phase change of Nano confined materials for the applications of thermal energy.

Mosavat et. al.[6] observed study of heat transfer of mechanical face seal and fin by using analytical method.Lin et. al.[7] introduced the concept of MHD unsteady flow of pseudo-plastic nanofluid andtransfer of heat in finite thin film with the generation of internal heatover stretching surface.Sheikholeslami et. al.[8] suggested the novel idea ofmagnetic fieldeffectson the unsteady flow of nano fluid and transfer of heat using Buongiorno model. Wang et. al. [9] investigatedheat transfer and fluid flow of nano particles of copper between two parallel porous plates having base fluid of water and ethylene–glycol. Bhattacharyya [10] discussed the stagnation-point of boundary layer flow of Casson fluid andtransfer of heat towards a shrinking or stretching sheet.Seth et. al.[11] proposed MHD flow of stagnation-point andtransfer of heat over non-isothermal shrinking or stretching sheet in a porous medium source effect.Nadeem et. al.[12] presented a numerical solution offlow of non-Newtonian nanofluid over stretching sheet.Kumaran et. al.[13] analyzed the computational analysis offlows ofMHD Casson and Maxwell fluids with cross diffusion. Hamid et. al.[14] observed shape effects of nano particles of MoS2 on rotating flow of nanofluid along a stretching sheet with changing thermal conductivity.Hayat et. al.[15] suggested analysis ofheat transfer and mass transfer in Maxwell fluid in the stagnation region over a stretched sheet.Usmanet. al.[16] gives the idea of Cu–Al2O3/water hybrid nanofluid in presence of nonlinear radiation and thermal conductivity.Bhattacharyya et. al.[17] presented transfer of reactive solute in MHD boundary layer flow over a stretched surface with suction or blowing.Akbar et. al.[18] analyzed tangent-hyperbolic fluidflow in inclined asymmetric channel with slip andtransfer of heat.Malik et. al.[19] suggested tangent-hyperbolic fluidMHD flow over a stretching cylinder by using the method of Keller box.Akbar et. al.[20] proposednumerical solution of boundary layer flow of MHDtangent-hyperbolic fluid past a stretching sheet.Hayat et. al.[21] presented tangent-hyperbolic fluid radiative flow in the presence of convective conditions.Usman et. al.[22] discussed the uniform heat fluxof Ferro fluids on its flow and heat transferalong a smooth plate.Nawaz et. al.[23] proposed study of finite element three dimensionalflow of radiative nano plasma by using Hall and ion slip currents.Nadeem et. al.[24] gave idea of analysis of nanoparticle forstagnation flow of non-orthogonal third order fluid towards a stretching sheet. Chamkha et. al.[25] presentedmixed convective flow in inclined square filled with nanofluid. Pedley et. al.[26] proposed Bio convective flow of a fluid. Kessler et. al.[27] observed growth of bioconvective patterns in presence of uniformly suspended gyrotactic microorganisms.Hillet. al.[28] discussedthe growth of bio convective patterns in the presence of gyrotactic microorganisms which are suspended in a layer of finite depth. Ghorai et. al.[29] proposed the development as well as stability of gyrotactic microorganisms in bioconvection. Makinde et. al.[30]presented the idea of boundary layer flow of nano fluid over a stretching sheet having convective boundary conditions.Jayalakshmiet. al.[31] discussedMHDmicropolarnanofluidoverpermeable stretching or shrinkingsheetin the presence

ofNewtonianheating.

3. METHODOLOGY

By above consideration, equations of thermal energy, total mass, momentum and microorganism can be found by nanofluid model as follows:

$$\nabla.\boldsymbol{u} = 0, \qquad \text{(III. 1)}$$

$$\rho\frac{d\boldsymbol{U}}{dt} = div\boldsymbol{\tau} + \{C\rho_p + [\rho_f(1-\beta(T-T_\infty))](1-C) - \gamma\Delta\rho N\}g_o + \sigma(\boldsymbol{J}\times\boldsymbol{B}), \qquad \text{(III. 2)}$$

$$\rho\frac{d\boldsymbol{e}}{dt} = \boldsymbol{\tau}.L - div\boldsymbol{q} + \boldsymbol{\tau}\left[D_B\nabla T.\nabla C + \left(\frac{D_T}{T_\infty}\right)\nabla T.\nabla T\right], \qquad \text{(III. 3)}$$

$$(\boldsymbol{u}.\nabla)C = D_B\nabla^2 C + \left(\frac{D_T}{T_\infty}\right)\nabla^2 T, \qquad \text{(III. 4)}$$

$$\nabla.\boldsymbol{j} = 0, \qquad \text{(III. 5)}$$

In above equations, $\boldsymbol{u} = (u, v, 0)$ is the velocity profile of nanofluid, T denotes temperature, C denotes concentration, N denotes concentration of microorganism, j denotes microorganism flux by diffusion, T_∞ denotes reference temperature, D_B denotes Brownian diffusion coefficient, D_T denotes thermophoretic diffusion coefficient,$\boldsymbol{J} = (\boldsymbol{V}\times\boldsymbol{B})$,$\boldsymbol{\tau}.L$ is viscous dissipation effect.

Microorganism flux j is represented by

$$\boldsymbol{j} = Nu + NV - D_n\nabla N$$

Here D_n denotes microorganism diffusivity and W_c denotes swimming speed of maximum cell.

As $\nabla = \left[\frac{\partial}{\partial x}, \frac{\partial}{\partial y}, \frac{\partial}{\partial z}\right]$ and $\boldsymbol{u} = (u, v, 0)$

By applying boundary layer assumption, above equations becomes

$$\frac{\partial u}{\partial x} + \frac{\partial v}{\partial y} = 0 \qquad \text{(III. 6)}$$

$$\frac{\partial u}{\partial t} + u\frac{\partial u}{\partial x} + v\frac{\partial u}{\partial y} = \upsilon(1-n)\frac{\partial^2 u}{\partial y^2} + \sqrt{2}\upsilon n\Gamma\frac{\partial u}{\partial y}\frac{\partial^2 u}{\partial y^2} - \frac{\sigma B^2}{\rho}u + [\beta\rho_{f\infty}(T-T_\infty)(1-C_\infty) - (\rho_p-\rho_{f\infty})(C-C_\infty) - \gamma(\rho_p-\rho_{f\infty})(N-N_\infty)]g_o \qquad \text{(III. 7)}$$

$$\frac{\partial T}{\partial t} + u\frac{\partial T}{\partial x} + v\frac{\partial T}{\partial y} = \frac{k}{\rho c_p}\left(\frac{\partial^2 T}{\partial y^2}\right) + \frac{Q}{\rho c_p}(T-T_\infty) + \frac{\mu}{\rho c_p}(1-n)\left(\frac{\partial u}{\partial y}\right)^2 + \frac{\mu n\Gamma}{\sqrt{2}\,\rho c_p}\left(\frac{\partial u}{\partial y}\right)^3 + \tau\left[D_B\frac{\partial T}{\partial y}\frac{\partial C}{\partial y} + \frac{D_T}{T_\infty}\left(\frac{\partial T}{\partial y}\right)^2\right] \qquad \text{(III. 8)}$$

$$\frac{\partial C}{\partial t} + u\frac{\partial C}{\partial x} + v\frac{\partial C}{\partial y} - \frac{D_T}{T_\infty}\left(\frac{\partial^2 T}{\partial y^2}\right) = D_B\frac{\partial^2 C}{\partial y^2} \qquad \text{(III. 9)}$$

$$-\frac{\partial N}{\partial t} + u\frac{\partial N}{\partial x} + v\frac{\partial N}{\partial y} = D_n\frac{\partial^2 N}{\partial y^2} \qquad \text{(III. 10)}$$

Boundary conditions

$$u = u_w,\ v = 0,\ T = T_w,\ C = C_w,\ N = N_w \text{ at } y = 0 \qquad \text{(III. 11)}$$

$$u \to 0, \quad T \to T_\infty, \quad C \to C_\infty, \quad N \to N_\infty \text{ as } y \to \infty \qquad \text{(III. 12)}$$

Using following similarity transformations

$$u = \frac{ax}{1-\varepsilon t}F'(\eta), \quad v = -\sqrt{\frac{av}{1-\varepsilon t}}F(\eta), \quad \eta = y\sqrt{\frac{a}{\upsilon(1-\varepsilon t)}}, \quad \theta(\eta) = \frac{T-T_\infty}{T_f-T_\infty}, \quad \phi(\eta) = \frac{C-C_\infty}{C_w-C_\infty}, \quad \xi(\eta) = \frac{N-N_\infty}{N_w-N_\infty}, \qquad \text{(III. 13)}$$

The above equations becomes,

$$(1-n)F'''(\eta) + nWeF''(\eta)F'''(\eta) - M^2F'(\eta) - F'^2(\eta) + F(\eta)F''(\eta) - A\left(F'(\eta) + \frac{\eta}{2}F''(\eta)\right) + [\theta - \phi N_r - \xi Rh_B]\beta = 0 \qquad \text{(III. 14)}$$

$$\frac{\theta''(\eta)}{Pr} + \lambda\theta(\eta) + Ec(1-n)F''^2(\eta) + \frac{n}{2}WeEcPrF''^3(\eta) - A\left(\frac{\eta}{2}\theta'(\eta) + \theta(\eta)\right) - F'(\eta)\theta(\eta) + F(\eta)\theta'(\eta) + N_b\theta'(\eta)\phi'(\eta) + N_t\theta'^2(\eta) = 0 \qquad \text{(III. 15)}$$

$$\phi''(\eta) + \frac{N_t}{N_b}\theta''(\eta) + \frac{1}{Sc}\left(F(\eta)\phi'(\eta) - \frac{\phi'(\eta)}{2}A\eta\right) = 0 \qquad \text{(III. 16)}$$

$$Sc_b\xi''(\eta) + \frac{\xi'(\eta)\eta A}{2} + F(\eta)\xi'(\eta) = 0 \qquad \text{(III. 17)}$$

Boundary conditions becomes

$$F'(\eta) = 1,\ F(\eta) = 0,\ \theta(\eta) = 1,\ \phi(\eta) = 1,\ \xi(\eta) = 1 \quad \text{as} \quad \eta \to 0$$

$$F'(\eta) \to 0,\ \theta(\eta) \to 0,\ \phi(\eta) \to 0,\ \xi(\eta) \to 0 \quad \text{as} \quad \eta \to \infty$$

A. Method of Solution

The governing equations {III.14} and {III.15} along with boundary conditions are highly nonlinear and complicated in nature so these are numerically solved

by using Runge-kutta Fehlberg method.

Let

$$F' = y_1, F'' = y_2, F''' = yy_1 \qquad (A.1)$$

$$\theta' = y_3\ , \theta'' = yy_2, \qquad (A.2)$$

Eq. {III.14} and {III.15}becomes

$$(1-n)yy_1 + nWey_2yy_1 + Fy_2 - {y_1}^2 - A\left(y_1 + \frac{\eta}{2}y_2\right) - M^2y_1 = 0 \qquad (A.3)$$

$$\frac{1}{Pr}yy_2 + Fy_3 - y_1\theta - A\left(\theta + \frac{\eta}{2}y_3\right) + \lambda\theta + Ecy_2{}^2 + \frac{n}{2}PrWeEcy_2{}^3 = 0 \qquad (A.4)$$

Boundary conditions are

$$F(0) = 0, y_1(0) = 1, \quad \theta(0) = 1. (A.5)$$

$$y_2(0) = S_1, y_3(0) = S_2. \quad (A.6)$$

4. RESULTS AND DISCUSSION

Graphical results and discussion section is dedicated to discover the influence of non-dimensional parameters on the behavior of velocity $\boldsymbol{F'(\eta)}$, temperature $\boldsymbol{\theta(\eta)}$, skin friction $\boldsymbol{C_f}$ and local heat flux $\boldsymbol{Nu_x}$. Two kinds of physical quantities i-e skin friction and reduced Nusselt number are also discussed to study the behavior of velocity and temperature distributions on the boundaries.

Figure IV.1shows the behavior of velocity distribution $\boldsymbol{F'(\eta)}$ verses magnetic field parameter $\boldsymbol{M}$ to distinct values of unsteadiness parameter$\boldsymbol{A}$. We see in the figure that decrease in velocity due to increase in$\boldsymbol{M}$. It is due to the fact that Hartmann number acts as the Lorentz force in the field which causes opposition in the velocity. So, increase in magnetic field $\boldsymbol{M}$ cause the increase in Lorentz force and as a result velocity declines. We can see drop in velocity is more for$\boldsymbol{A}$ =0 as that for $\boldsymbol{A}$ =1.

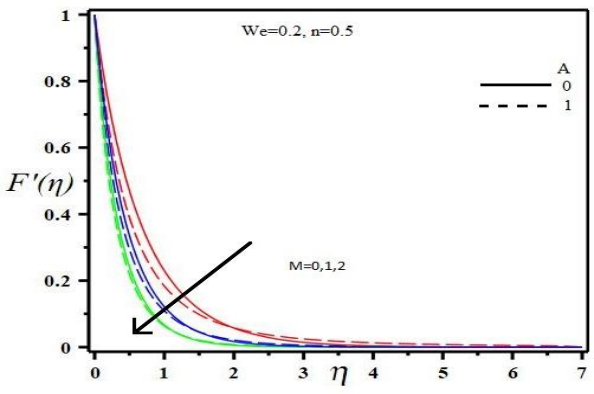

Figure 0-1: Velocity distribution F′($\boldsymbol{\eta}$) verses $\boldsymbol{M}$ to different values of $\boldsymbol{A}$

Figure IV.2 exhibits the behavior of power-law index $\boldsymbol{n}$ on velocity distribution $\boldsymbol{F'(\eta)}$ to distinct values of unsteadiness parameter$\boldsymbol{A}$. In this figure, we see that as the values of$\boldsymbol{n}$ increases, the velocity decreases. This behavior is due to Hartmann number $\boldsymbol{M}$ acting as a Lorentz force which in turn opposes the velocity distribution. Also, for $\boldsymbol{A}$ =0, the decrease in velocity is less and for $\boldsymbol{A}$ =1, the decrease in velocity is more.

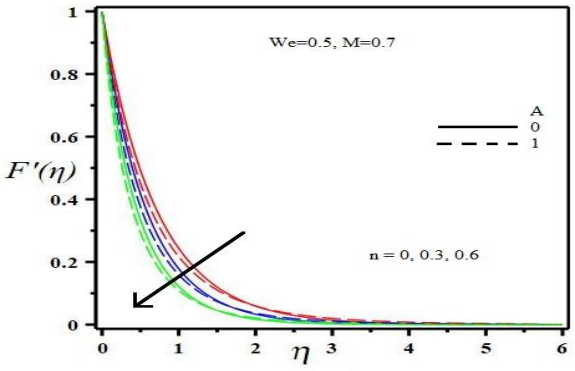

Figure 0-2: Velocity distribution $\boldsymbol{F'(\eta)}$verses$\boldsymbol{n}$ to distinct values of $\boldsymbol{A}$

Figure IV.3 is showing the behavior of velocity distribution $\boldsymbol{F'(\eta)}$ verses Weissenberg number $\boldsymbol{We}$ to the various values of unsteadiness parameter $\boldsymbol{A}$. A consistent decrease in velocity is seen when the value of Weissenberg number $\boldsymbol{We}$ is increased. The physical reasoning is due to the drag force which appears between the layers of the fluid due to the presence of magnetic field. Weissenberg number $\boldsymbol{We}$ is defined as the ratio of relaxation time to that of process time. Physically, $\boldsymbol{We}$ enhances thickness of the fluid which causes in the decline of velocity of the fluid. Also, for $\boldsymbol{A}$ =0, velocity decrease is less as that for $\boldsymbol{A}$ =1.

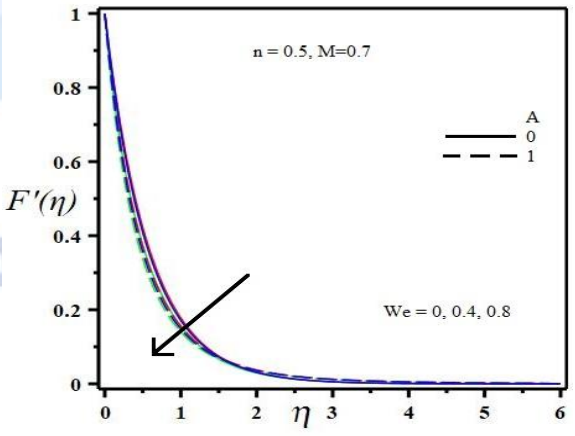

Figure 0-3: Velocity distribution $\boldsymbol{F'(\eta)}$verses $\boldsymbol{We}$ to distinct values of $\boldsymbol{A}$

Figure IV.4 bespeaks the consequences of Prandtl number $\boldsymbol{Pr}$ to that of temperature distribution $\boldsymbol{\theta(\eta)}$ to distinct values of unsteadiness parameter $\boldsymbol{A}$. As Prandtl number $\boldsymbol{Pr}$ is defined as the ratio of the diffusivity of momentum to that of thermal diffusivity. So increasing Prandtl number cause the decrease in temperature due to the inverse relation of $\boldsymbol{Pr}$ and thermal diffusivity. Also for $\boldsymbol{A}$ =0, decrease in temperature is more as that for $\boldsymbol{A}$ =1.

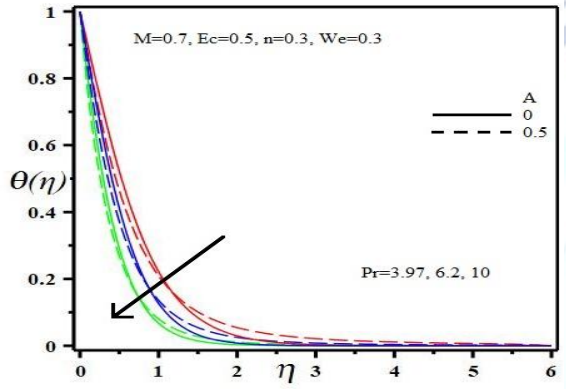

Figure 0-4: Temperature distribution $\boldsymbol{\theta(\eta)}$ verses$\boldsymbol{Pr}$ to distinct values of $\boldsymbol{A}$

Figure IV.5 explores temperature distribution $\boldsymbol{\theta(\eta)}$ verses Eckert number$\boldsymbol{Ec}$ to distinct values of heat source parameter$\boldsymbol{\lambda}$. As Ec measures the kinetic energy of fluid flow relative to the enthalpy difference. So increasing the $\boldsymbol{Ec}$ causes increase in kinetic energy. Physically, heat dissipation increases due to increased collision of particles of fluid. This dissipated heat is added to the system again which causes increase in the temperature. For$\boldsymbol{\lambda}$ = 0, decrease in temperature distribution is more and for $\boldsymbol{\lambda}$ = 0.2, decrease in temperature distribution is less.

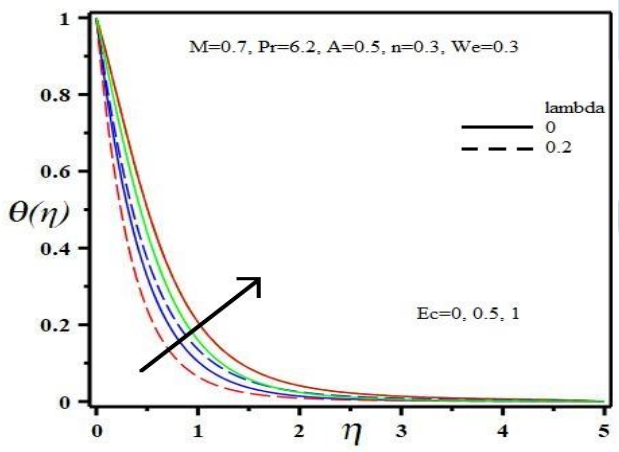

Figure 0-5: Temperature distribution $\boldsymbol{\theta(\eta)}$verses $\boldsymbol{Ec}$ to distinct values of $\boldsymbol{\lambda}$

Figure IV.6 exhibits the behavior of skin friction $\boldsymbol{C_f}$verses Weissenberg number $\boldsymbol{We}$ to the distinct values of magnetic field parameter $\boldsymbol{M}$. Enhancement in values of $\boldsymbol{We}$ causes decrease in skin friction because $\boldsymbol{We}$ increases the thickness of the fluid which results in the decrease in skin friction. Similarly, increasing Hartmann number $\boldsymbol{M}$ gives decrease in skin friction. Also, as the unsteadiness parameter increases, the value of coefficient of skin friction increases.

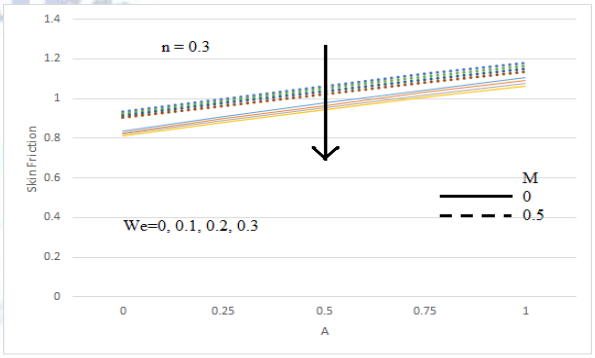

Figure 0-6: Coefficient of skin friction $\boldsymbol{C_f}$ verses $\boldsymbol{We}$ to distinct values of $\boldsymbol{M}$

Figure IV.7 depicts the effect of Weissenberg number $\boldsymbol{We}$ on the skin friction $\boldsymbol{C_f}$ to the distinct values of power-law index$\boldsymbol{n}$. Increasing the Weissenberg number $\boldsymbol{We}$ causes the drop in skin friction. For smaller values of$\boldsymbol{n}$, skin friction is more and for larger values of$\boldsymbol{n}$, skin friction is less. Also, increasing unsteadiness parameter $\boldsymbol{A}$ results in the increasing skin friction.

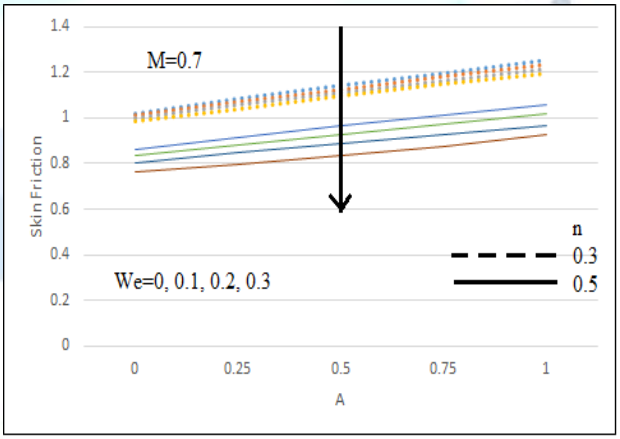

Figure 0-7: Coefficient of skin friction $\boldsymbol{C_f}$ verses $\boldsymbol{We}$ to distinct values of $\boldsymbol{n}$

Figure IV.8 shows the influence of Eckert Number $\boldsymbol{Ec}$ to the reduced Nusselt number $\boldsymbol{Nu_x}$ to the distinct values of heat source parameter $\boldsymbol{\lambda}$. As Eckert number $\boldsymbol{Ec}$ is risen-up, reduced Nusselt number is dropped. For the increasing values of unsteadiness parameter $\boldsymbol{A}$ gives

increase in reduced Nusselt number.

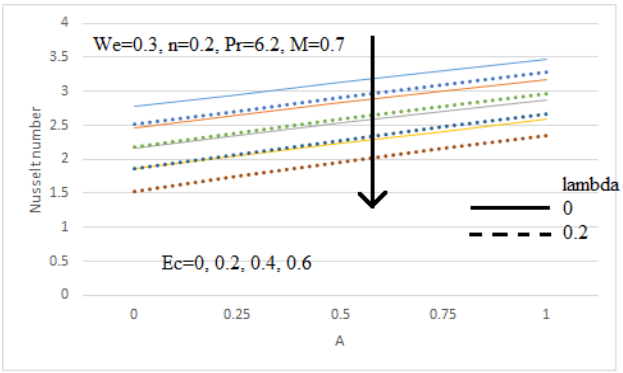

Figure 0-8: Nusselt number Nu_x verses Ec to distinct values of λ

Figure IV.9 bespeaks about the reduced Nusselt number Nu_x and the power law index n to various values of Prandtl numberPr. Reduced Nusselt number Nu_x increases when Prandtl number Pr is increased. Also, enhancing unsteadiness parameter, causes enhancement in reduced Nusselt number.

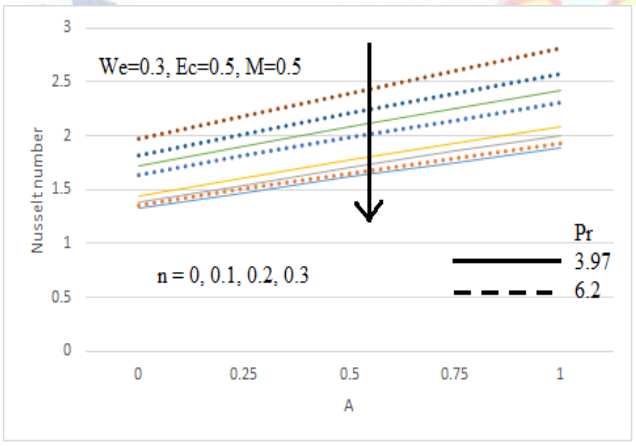

Figure 0-9: Nusselt number Nu_x verses n to distinct values of Pr

Figure IV.10 is constructed to show the comparison of coefficient of skin friction with the existing literature when $We = 0$, $n = 0$ and for various values of$M$. The results are showing the excellent agreement with the paper results.

M	C_f				
	[28]	[36]	[37]	Paper results	Review results
0	1	1	1	1	1
1	-1.41421	-1.41421	-1.41421	-1.41421	-1.4141
5	-2.44948	-2.44948	-2.44948	-2.44948	-2.44945
10	-3.31662	-3.31662	-3.31662	-3.31662	-3.31662
50	-7.14142	-7.14142	-7.14142	-7.14142	-7.14142
100	10.0499	10.0499	10.0499	10.0499	10.0499
500	-22.3830	-22.3830	-22.3830	-22.3830	-22.3830
10000	31.6383	31.6383	31.6383	31.6383	31.6383

Figure 0-10: Comparison of present results of coefficient of skin friction with previously published data when We=0, n=0 and for different values of M

Figure IV.11 is constructed to show the comparison of coefficient of skin friction with the existing literature when We=0, 0.3, 0.5 and for the various values of M and$n$. It is observed that increasing the values of M gives more accuracy as that of smaller values of$M$.

n, M	We = 0.0			We = 0.3			We = 0.5		
	[28]	Paper results	Review results	[28]	Paper results	Review results	[28]	Paper results	Review results
0, 0	1	1	1	1	1	1	1	1	1
0.1, 0	0.94868	0.94868	0.94868	0.94868	0.94868	0.94868	0.94868	0.94868	0.94868
0.2, 0	0.89442	0.89442	0.89442	0.89442	0.89442	0.89442	0.89442	0.89442	0.89442
0.3, 0.5	1.09544	1.09544	1.09544	1.09544	1.09544	1.09544	1.09544	1.09544	1.09544
0.3, 1	1.26491	1.26491	1.26491	1.26491	1.26491	1.26491	1.26491	1.26491	1.26491
0.3, 1.5	1.41421	1.41421	1.41421	1.41421	1.41421	1.41421	1.41421	1.41421	1.41421

Figure 0-11: Comparison of coefficient of skin friction with previously published data for different values of M, n and We.

5. CONCLUSION

A Bio convective flow of a nano fluid past a stretching sheet has been investigated in this chapter. Gyrotactic microorganisms are added along with nano particles within the base fluid. The governing problem flow is tackled numerically to explore velocity $F'(\eta)$, temperature $\theta(\eta)$, concentration $\phi(\eta)$, motile microorganism density $\xi(\eta)$, Nusselt number Nu_x, Sherwood number Sh_x and local motile microorganism density parameter Nn_x against pertinent physical parameters. The main outcomes of this chapter can be summarized as:

- Schmidt number Sc makes the velocity profile$F'(\eta)$ to dropalong with magnetic parameter M but temperature $\theta(\eta)$, concentration $\phi(\eta)$ and motile microorganism density$\xi(\eta)$ are enhanced.
- Velocity profile$F'(\eta)$ decreases by increasing Bio convection Lewis parameter Sb while temperature $\theta(\eta)$

and motile microorganism density $\xi(\eta)$ are enhanced. But there is no visible effect on concentration profile $\phi(\eta)$.

- Velocity profile $F'(\eta)$ decreases by rising Buoyancy ratio parameter Nr but temperature $\theta(\eta)$ and motile microorganism density $\xi(\eta)$ are enhanced. Also, there is slight increasing effect on concentration profile $\phi(\eta)$.
- By raising the values of Thermophoresis parameter Nt makes the temperature $\theta(\eta)$, concentration $\phi(\eta)$ and motile microorganism density $\xi(\eta)$ to enhance.
- Increasing the values of Brownian motion parameter Nb makes velocity $F'(\eta)$ to decrease but the temperature $\theta(\eta)$ and concentration $\phi(\eta)$ are increased. There is no visible effect on motile microorganism density $\xi(\eta)$.
- Increasing bio convection Rayleigh number Rb makes temperature $\theta(\eta)$, concentration $\phi(\eta)$ and motile microorganism density $\xi(\eta)$ to enhance.
- Reduced Nusselt number Nu_x is increasing for Schmidt number Sc and Thermophoresis parameter Nt but decreasing for bio convection Rayleigh number Rb, Brownian motion parameter Nb , Buoyancy ratio parameter Nr and Bio convection Lewis parameter Sb.
- Sherwood number Sh_x and motile microorganism density Nn_x are showing an increasing effect for Thermophoresis parameter Nt and decreasing effect for other parameters.

6. FUTURE WORK

The present research work aims to investigate the flow of tangent-hyperbolic fluid past a stretching sheet. Unsteady flow and heat transfer was discussed in the presence of MHD. Tangent-hyperbolic fluid flow over a horizontal stretching sheet was discussed in the presence of MHD in the analysis which is the review work of Usman et al. An effort was made to extend the work done in chapter two by considering the bio convection nano fluid at the flat surface of tangent-hyperbolic fluid. This work may be extended by considering the viscous dissipation, velocity slip, non-Fourier heat flux and thermal radiation effects

Conflict of interest statement

Authors declare that they do not have any conflict of interest.

REFERENCES

[1] Besthapu P, Haq RU, Bandari S, Al-mdallal QM. Mixed convection flow of thermally stratified MHD nanofluid over an exponentially stretching surface with viscous dissipation effect. J Taiwan Inst Chem Eng. 2017;71:307-314.

[2] Sheikholeslami M, Rokni HB. Magnetic nanofluid flow and convective heat transfer in a porous cavity considering Brownian motion effects. Phys Fluids. 2018;30(1):012003.

[3] Sheikholeslami M. Numerical approach for MHD Al2O3–water nanofluid transportation inside a permeable medium using innovative computer method. Comput Methods Appl Mech Eng. 2019;344:306-318.

[4] Sheikholeslami M. New computational approach for energy and entropy analysis of nanofluid under the impact of Lorentz force through a porous media. Comput Methods Appl Mech Eng. 2019;344:319-333.

[5] Aftab W, Huang X, Wu X, Liang Z, Mahmood A, Zou R. Nano confined phase change materials for thermal energy applications. Energy Environ Sci. 2018;11(6):1392-1424.

[6] Mosavat M, Moradi R, Takami MR, Gerdroodbary MB, Ganji DD. Heat transfer study of mechanical face seal and fin by analytical method. Eng Sci Technol Int J. 2018;21(3):380-388.

[7] Lin Y, Zheng L, Zhang X, Ma L, Chen G. MHD pseudo-plastic nanofluid unsteady flow and heat transfer in a finite thin film over stretching surface with internal heat generation. Int J Heat Mass Transfer. 2015;84: 903-911.

[8] Sheikholeslami M, Ganji DD, Rashidi MM. Magnetic field effect on unsteady nanofluid flow and heat transfer using Buongiorno model. J Magn Mater. 2016;416:164-173.

[9] Usman M, Hamid M, Haq RU, Wang W. Heat and fluid flow of water and ethylene–glycol based Cu-nanoparticles between two parallel squeezing porous disks: LSGM approach. Int J Heat Mass Transfer. 2018;123:888-895.

[10] Bhattacharyya K. Boundary layer stagnation-point flow of Casson fluid and heat transfer towards a shrinking/stretching sheet. Front Heat Mass Transfer (FHMT). 2013;4(2). http://doi.org/10.5098/hmt.v4. 2.3003

[11] Seth GS, Singha AK, Mandal MS, Banerjee A, Bhattacharyya K. MHD stagnation-point flow and heat transfer past a non-isothermal shrinking/stretching sheet in porous medium with heat sink or source effect. Int J Mech Sci. 2017;134:98-111.

[12] Nadeem S, Haq RU, Khan ZH. Numerical solution of non-Newtonian nanofluid flow over a stretching sheet. Appl Nanosci. 2014;4(5):625-631.

[13] Kumaran G, Sandeep N, Ali ME. Computational analysis of magneto hydrodynamic Casson and Maxwell flows over a stretching sheet with cross diffusion. Results Phys. 2017;7:147-155.

[14] Hamid M, Usman M, Zubair T, Haq RU, Wang W. Shape effects of MoS2 nano-particles on rotating flow of nanofluid along a stretching surface with variable thermal conductivity: a Galerkin approach. Int J Heat Mass Transfer. 2018;124:706-714.

[15] Hayat T, Khan MI, Imtiaz M, Alsaedi A. Heat and mass transfer analysis in the stagnation region of Maxwell fluid with chemical reaction over a stretched surface. J Therm Sci Eng Appl. 2018;10(1):011002.

[16] Usman M, Hamid M, Zubair T, Haq RU, Wang W. Cu–Al2O3/water hybrid nanofluid through a permeable surface in the presence of nonlinear radiation and variable thermal conductivity via LSM. Int J Heat Mass Transfer. 2018;126:1347-1356.

[17] Bhattacharyya K, Mukhopadhyay S, Layek GC. Reactive solute transfer in magneto hydrodynamic boundary layer stagnation-point flow over a stretching sheet with suction/blowing. Chem Eng Commun. 2012;199(3): 368-383.

[18] Akbar NS, Hayat T, Nadeem S, Obaidat S. Peristaltic flow of a tangent hyperbolic fluid in an inclined asymmetric channel with slip and heat transfer. Prog Comput Fluid Dyn Int J. 2012;12(5):363-374.

[19] Malik MY, Salahuddin T, Hussain A, Bilal S. MHD flow of tangent hyperbolic fluid over a stretching cylinder: using Keller box method. J Magn Magn Mater. 2015;395:271-276.

[20] Akbar NS, Nadeem S, Haq RU, Khan ZH. Numerical solutions of magneto hydrodynamic boundary layer flow of tangent hyperbolic fluid towards a stretching sheet. Indian J Phys. 2013;87(11):1121-1124.

[21] Hayat T, Qayyum S, Ahmad B, Waqas M. Radiative flow of a tangent hyperbolic fluid with convective conditions and chemical reaction. Eur Phys J Plus. 2016;131(12):422.

[22] Usman M, Hamid M, Mohyud-din ST, Waheed A, Wang W. Exploration of uniform heat flux on the flow and heat transportation of Ferro fluids along a smooth plate: comparative investigation. Int J Bio math. 2018 ; 11(2):1850048.

[23] Nawaz M, Zubair T. Finite element study of three dimensional radiative nano-plasma flow subject to Hall and ion slip currents. Results Phys. 2017;7:4111-4122.

[24] S. Nadeem, R. Mehmood, N.S. Akbar. Nanoparticle analysis for non-orthogonal stagnation point flow of a third order fluid towards a stretching surface. Journal of Computational and Theoretical Nano science, 10 (2013), pp. 2737-2747

[25] E. Abu-Nada, A.J. Chamkha. Mixed convection flow in a lid-driven inclined square enclosure filled with a nanofluid. European Journal of Mechanics-B/Fluids, 29 (2010), pp. 472-482

[26] N. Hill, T. Pedley. Bio convection. Fluid Dyn. Res., 37 (2005), p. 1

[27] T.J. Pedley, N.A. Hill, J.O. Kessler, The growth of bioconvection patterns in a uniform suspension of gyrotactic microorganisms. J. Fluid Mech. 195, 223–237(1988)

[28] N.A. Hill, T. J. Pedley, J.O. Kessler, Growth of bioconvection patterns in a suspension of gyrotactic microorganisms in a layer of finite depth. J. Fluid Mech. 208, 509–543(1989)

[29] S. Ghorai, N.A. Hill, Development and stability of gyrotactic plumes in bioconvection. J. FluidMech.400, 1–31 (1999)

[30] O.D. Makinde, A. Aziz. Boundary layer flow of a nanofluid past a stretching sheet with a convective boundary condition. Int. J. Therm. Sci., 50 (2011), pp. 1326-1332

[31] K.Gangadhar, T. Kannan, P. Jayalakshmi, Magne to hydro dynamic micro polarnano fluid pastapermeable stretching/ shrinking sheet with Newton ian heating.J.Braz.Soc.Mech.Sci.Eng.39,4379–4391(2017)